INVITED PAPER *Special Section on Antenna and Propagation Technologies Contributing to Realization of Next Generation Wireless Systems*

Novel Cellular Active Array Antenna System at Base Station for Beyond 4G

Masayuki NAKANO[†a)], ***Senior Member***

SUMMARY This paper introduces a base station antenna system as a future cellular technology. The base station antenna system is the key to achieving high-speed data transmission. It is particularly important to improve the frequency reuse factor as one of the roles of a base station. Furthermore, in order to solve the interference problem due to the same frequency being used by the macro cell and the small cell, the author focuses on beam and null control using an AAS (Active Antenna System) and elucidates their effects through area simulations and field tests. The results showed that AAS can improve the SINR (signal to interference-plus-noise ratio) of the small cell area inside macro cells. The paper shows that cell quality performance can be improved by incorporating the AAS into a cellular base station as its antenna system for beyond 4G radio access technology including the 5G cellular system.

key words: *active antenna system, null, cellular, base station antenna, small cell*

1. Introduction

There is demand for a high-speed data service for the next-generation cellular systems. The technology requires not only wider bandwidth and higher frequency, but the cell radius also needs to be reduced, e.g., to pico cells and femto-cells. Moreover, the cell shape changes from 2-dimensional (=2D) to 3-dimensional (=3D) due to the need to reach tall buildings, high overpass roads, etc. from ground level. On this basis, it is clear that antenna technology is the most fundamental and crucial factor to covering a 3D area.

Firstly, one example of this antenna technology is a MIMO (Multiple-Input Multiple-Output) technique. MIMO technology can increase the data rate by using multiple antennas. Conventional two-branch MIMO could be easily implemented by a single antenna using orthogonal polarization [1]. On the other hand, for three branch MIMO (or more), more antenna poles are needed [2]. This is very expensive, resulting in high CAPEX levels. Therefore, it is important that the base station antenna technology develops in the direction of miniaturization and aggregation.

Secondary, in order to use the broadband frequency, the frequency is much higher, so it is particularly important to adopt the millimeter wave. A millimeter wave antenna is smaller than a microwave antenna, thereby enabling compact and straightforward implementation in the base station. It needs to include many array elements and use microfabrication [3].

Manuscript received May 13, 2016.
Manuscript revised September 18, 2016.

[†]The author is with KDDI R&D Laboratories Inc., Fujimino-shi, 356-8502 Japan.
a) E-mail: m-nakano@m.ieice.org

DOI: 10.1587/transcom.2016WSI0001

Thirdly, metamaterial technology is an attractive new development. FSS (frequency selective surface) and EBG (electromagnetic band gap) have useful characteristics for various antenna patterns. Reference [4] shows that by using multiple woodpile metamaterial reflectors and a radiator, it is possible to establish the same beamwidth for a triple-frequency band. Further, Ref. [5] shows an array antenna using woodpile EBG in order to realize a higher gain. Next, Refs. [6], [7] show a strip-type composite right/left-handed line with a downtilted beam. Using an EBG/AMC (artificial magnetic conductor) structure of dual-frequency phased array antennas, a study was performed to reduce the size of the lower band element and decrease the coupling of the higher band [8]. Reference [9] used simulation and experiments to show that a cylindrical EBG controlled with PIN diodes is able to act as azimuth beam steering. Also, K. Cho, et al. demonstrated in their study the beamwidth of a dipole antenna with a frequency selective reflector using dual-frequency band elements [10]. From the above-mentioned study examples, FSS and EBG are regarded as the promising technologies for next-generation base station antennas, for which many of the current antenna characteristics are altered.

Finally, Massive MIMO is one of the most anticipated developments of future technology [11]. Many studies have been conducted. H. Papadopoulos et al. report on Massive MIMO activities in relation to 5G, including standardization efforts and system development [12]. On the other hand, it will be difficult in the near future to mount everything digitally, such as components like an AD/DA converter in order to avoid high costs and excess heat. Thus, it has been proposed that a hybrid of analog and digital technology be adopted [13]. Further, in the case of a base station system using multiple antenna elements such as Massive MIMO at high frequency, there is a large number of RF cables from the antennas to the radio equipment, making the RF power very lossy. Therefore, an AAS (active antenna system), which is unified and compact with an antenna element and an active device like an amplifier, is the aim of current developments and research. The AAS has a function that reduces the infrastructure cost and improves the quality of the area under beam control.

Currently, a study on shaped beam antennas aimed at cell quality improvement has been carried out [14]. A shaped beam antenna can reduce the radio interference between sectors on the site. Moreover, this is expected to improve the radio cell quality in the case of small cells, e.g., a pico cell

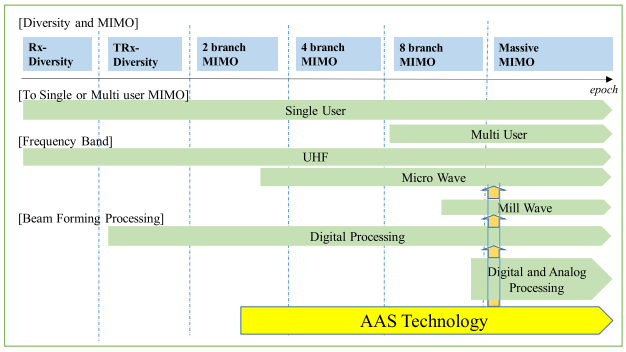

Fig. 1 Road Map of Antenna-related Technologies.

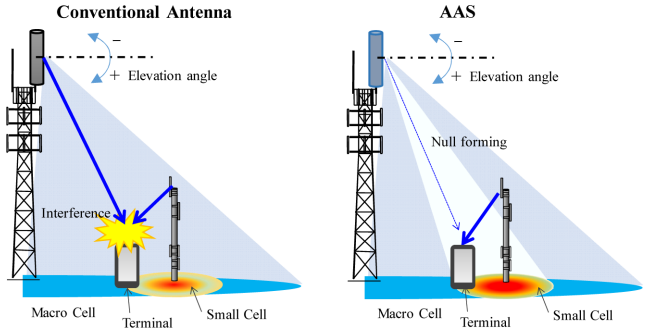

Fig. 2 Diagram of beam and null control for small cells using AAS.

inside a macro cell in the so-called Heterogeneous Network. Reference [15] shows that if the position of the small cell inside the macro cell changes, the radio cell quality of the macro cell is affected. Further, Ref. [16] shows that in areas where macro cells and small cells are mixed, the radio cell quality is evaluated using a 3D antenna pattern at the base station. As a result, narrowing the beamwidth on the vertical plane has been shown to be effective.

Figure 1 shows a road map of the various antenna-related technologies based on the evaluation of the antenna diversity and MIMO. In the future, antenna diversity technology is moving in the direction of Massive MIMO. On the other hand, AAS technology already existed in order to make the antenna compact to enable connection to an RF active device. Massive MIMO requires RF active devices per antenna element. Therefore, AAS technology has been in the spotlight again for the utilization of micro- and millimeter-waves. AAS has become the most important fundamental technology to achieve beyond 4G networks including the 5G cellular system.

This paper focuses on the cell quality performance by incorporating the AAS into the cellular base station as its antenna system for beyond 4G radio access technology. The remainder of this paper is organized as follows. Section 2 describes the characteristics of the base station antenna using the proposed AAS. Section 3 presents the general area performance results obtained from the simulation. Section 4 shows the performance of the proposed AAS in outdoor field tests. Finally, Sect. 5 concludes the paper.

2. Active Antenna System

Generally, in the future, in many of the uses of base station antennas, the interference reduction effect will be the most important aspect. In particular, dynamic area control during same frequency reuse is expected. The author believes that AAS technology is the most effective way to solve this problem. By suppressing the coaxial cable losses, the AAS was shown to improve the transmission output power of the downlink during field tests by 4 dB [17]. When a 4-element base station antenna uses an RF-MEMS (Radio Frequency-Micro Electro Mechanical System) device, the tilt angle changes to 9 degrees in the vertical plane [18]. In addition, there has been discussions on AAS features such as self-healing [19] and radio measurement methods using OTA (over the air) [20]. Finally, the author carries out field evaluations of cell quality using the AAS with beam control as part of the experiments and simulations [21].

An AAS involves the close integration of antennas with radio equipment. This boosts the communication coverage area, while reducing power consumption and overall size. Also, an AAS can achieve lower construction costs than existing non-integrated antennas. Some of the advantages of AAS are expected to be even greater at higher frequencies because the cable loss is greater at these frequencies. The AAS will be incorporated into 4G or beyond 4G mobile communication systems owing to an increase in the feeder loss and in the propagation loss at higher frequencies, degradation of the receiving sensitivity by an inferior noise figure (NF) or an increase in the transmission power because loss compensation may be used. An AAS in which the front-end circuits are placed directly beneath each antenna element is considered as the one of the solutions to these problems. In a beyond 4G system, it can be expected that the coverage area will be significantly improved due to the introduction of an AAS.

By using the AAS to transmit a null pattern toward the small cells existing within the macro cell, same frequency interference between the macro cells and small cells can be reduced, as is shown in the diagram in Fig. 2. The figure on the left (a) shows the use of a conventional antenna; the figure on the right (b) shows the use of beam and null control in the AAS. In this way, it is expected that AAS can reduce interference between a macro cell and small cell operating on the same frequency.

3. Simulation Evaluation

In this section, in order to evaluate some of the effects of the AAS, an area simulation is performed. In this simulation, four kinds of antenna patterns are used. The first is the "Standard Pattern", with no null pattern transmission to the small cell, where the Standard Pattern is almost the same as the conventional pattern [22]. This pattern has a low upper sidelobe and 1st null fill to the ground, which are characteristics of a typical base station antenna. The second

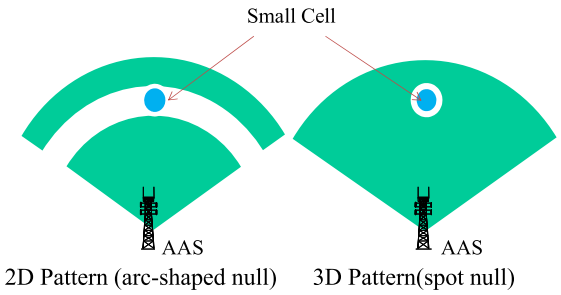

Fig. 3 Null patterns in coverage area.

"2D Pattern" is an arc-shaped null pattern. The third pattern is the "3D Pattern", which is a spot null pattern using vertical and horizontal arrays. Lastly, the "3D Pattern-Wide" has a wider null pattern than the 3D Pattern. However, the null depth of the 3D Pattern-Wide is shallower than in the 3D Pattern.

The array structure consists of 12 elements in the vertical plane. The number of the elements in the horizontal plane is 1 for the 2D Pattern and 4 for the 3D Pattern. Furthermore, the antenna pattern of the 2D Pattern is generated by the algorithm presented in next section. The antenna pattern of the 3D Pattern is generated by the classical technique using a sidelobe canceller. First, in order to make the sidelobe, a 4x4 sub-array. This sub-array is able to form the spot beam. Second, by combining the 8x4 array and 4x4 sub-array with opposite phases, it is possible to form a spot null pattern.

Figure 3 shows the null areas for the 2D Pattern and the 3D Pattern. Each pattern is shown in Fig. 4. Figure 4(a) shows the pattern in the vertical plane, in the direction of 15 degrees for the null pattern transmission to the small cell. Figure 4(b) is the pattern in the horizontal plane at 15 degrees on the vertical plane. The gain of the 2D Pattern is low in all directions, and as a result, the 2D Pattern formed an arc-shape as the null area. The 3D Pattern forms a null in the direction of 0 degree to the azimuth; as a result, there is a null spot in that area. Figure 4(c) shows the horizontal pattern at maximum radiation directional (5 degrees) to the vertical plane. The case of these Standard Pattern, 2D Pattern and 3D Pattern are the commonly used patterns for a small cell base station that is omni-directional in the horizontal plane and at 45 degrees of tilt in the vertical plane.

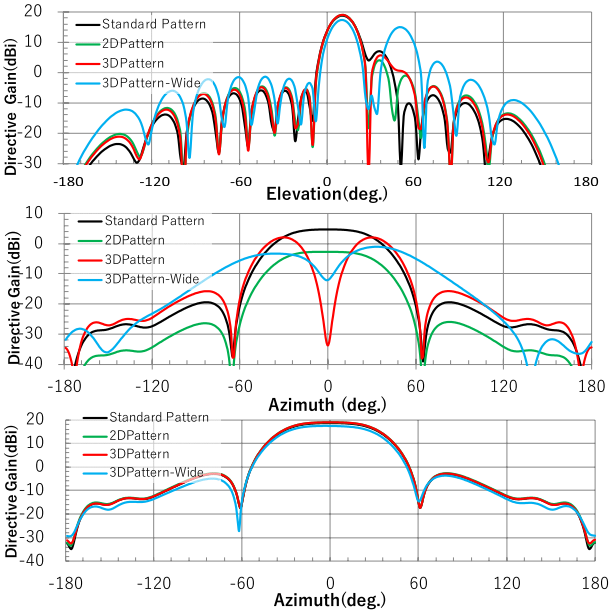

Fig. 4 Antenna pattern of AAS.
top :(a) in vertical plane
center: (b) in conical plane at elevation 15 degrees
bottom:(c) in conical plane at elevation 5 degrees

Table 1 Simulation conditions and parameters.

Cell Architecture	Frequency	3.5 GHz
	Cell Allocation	3 sector/cell
	Cell Radius	600 m
	Direction of Sector	90 deg., 210 deg., 330 deg.
	Region of Observation	radius 200 m from center cell
Macro cell Base Station	Antenna Height	30 m
	Propagation	Walfisch-Ikegami
	Building Interval, Width of Road, Average Building Height, Street Orientation Angle	20.6 m, 17.7 m, 13 m, 45 deg.
	Output Power	39.6 dBm
	Antenna Gain	20 dBi
Small Cell Base Station	Propagation Loss	3.5 low
	Antenna Height	5 m
	Output Power	36 dBm
	Antenna Gain	2 dBi
Terminal Station	Pattern	Omni-directional
	Antenna Height	1.5 m
	Antenna Gain	0 dBi

3.1 Simulation Result

The simulation conditions and parameters are shown in Table 1. The simulation scenario is that the small cell is located 115 m away from the AAS and in the main beam direction from the AAS in the horizontal plane. This point is positioned in the spot null for the 3D Pattern. The radius of the cell is set at 600 m. On the other hand, the radius of the observation region from the center macro cell is set at 200 m to clarify the performance of the null control effect on near the small cell. As a result, it is possible to ignore the interference from the neighbor cells. Therefore, the cell allocation is selected by 3 sector/cell only.

Figure 5 shows the SINR distribution results from the simulation with the AAS only and without the small cell. In all figures, the SINR at the sector boundary is equal to or less than 0 dB. For the 2D Pattern, it can be seen that the SINR is degraded into the arc shape. In the 3D Pattern, a spot-like SINR degradation point can be seen. For the 3D Pattern-Wide, a large decrease in SINR can be seen surrounding the location allocated for the small cell.

Figure 6 shows the SINR distribution for an AAS with small cells. In comparison with the Standard Pattern, the

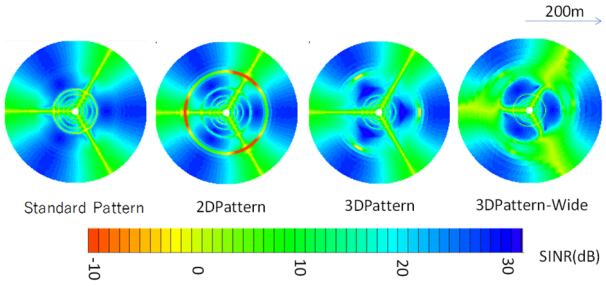

Fig. 5 SINR distribution (without small cell).

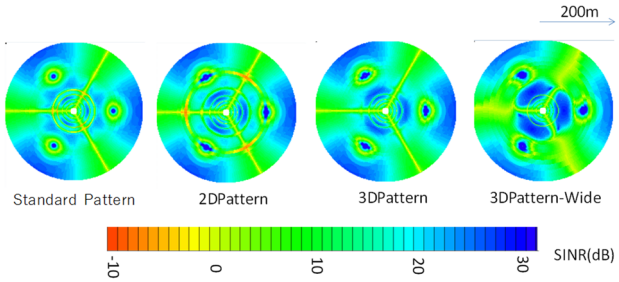

Fig. 6 SINR distribution (with small cell).

Table 2 Average of SINR and percentage of terminals in small cell.

		Standard Pattern	2D Pattern	3D Pattern	3D Pattern-Wide
Without Small Cell	SINR (dB)	18.4	-	-	-
With Small Cell	SINR (Macro + Small) (dB)	15.4	14.7	15.8	13.4
	SINR (Macro)	15.6	15.2	15.9	13.4
	SINR (Small Cell) (dB)	9.0	9.31	15.2	13.9
	Percentage of terminals in Small Cell (%)	3.30	7.59	3.88	6.2

SINR distribution around the small cells for the 2D Pattern, 3D Pattern and 3D Pattern-wide are higher and broader.

Table 2 shows the SINR in the macro and small cell areas, the SINR in the macro area only, the SINR in the small cell area only and the percentage of terminals that can be allocated in the small cell area. If the value of this percentage is large, even without improvements to SINR, the load on the macro cell can be reduced. Table 2 shows the best SINR is achieved where there is no small cell because there is no interference from the small cell. However, in order to increase cell capacity, the small cell has to be allocated in the macro cell. Therefore, by arranging the position of the small cell, the designs having a high SINR can be evaluated. The SINR of the AAS with the small cell (15.4 dB) is 3 dB less than the SINR without the small cell (18.4 dB) when the Standard Pattern is used. This is due to same frequency interference between the AAS and the small cell. Comparing the Standard Pattern with the 3D Pattern, the SINR for the entire (= macro and small) AAS and the small cell is nearly equal; on the other hand, the SINR for the small cell is improved by approximately 6 dB from 9.0 dB to 15.2 dB.

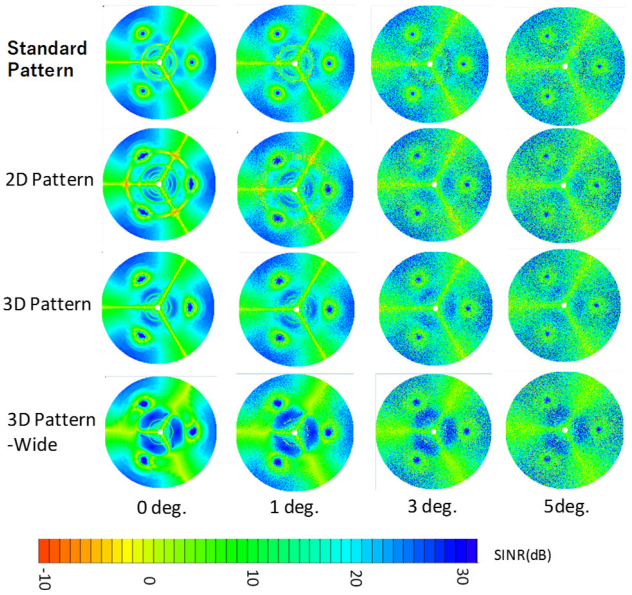

Fig. 7 SINR distribution with angular spread.

In addition, the SINR is nearly equal for the Standard Pattern and the 2D Pattern, however, for the 2D Pattern, the percentage of terminals that can be allocated in the small cell area is doubled, from 3.3% to 7.6%. Therefore, these changes can be expected to improve load balancing in a cellular network.

Comparing the 3D Pattern with the 3D Pattern-Wide, the SINR of the 3D Pattern is 1~2 dB higher than that for the 3D Pattern-Wide. On the other hand, the percentage of terminals for the 3D Pattern-Wide is approx. 2% (=6.2-3.85) more than that for the 3D Pattern. Therefore, the 3D Pattern-Wide can also be expected to contribute to balancing in a cellular network.

3.2 Evaluation with Angular Spread

In general, reflection, diffraction, scattering from buildings and so on means the antenna pattern of the base station antenna will not be directly received on the ground. To account for this effect, a simulation using an antenna pattern with a spatial angular spread as parameters was performed. The parameter values of the angular spread are 0, 1, 3, and 5 degrees; these values replicate the conditions for an open area, sub-urban, urban, and dense urban areas. Figure 7 shows the SINR distribution with angular spreads. In these figures, as the angular spread increases, the SINR distribution becomes lighter. As a result, it can be seen that the proportion of high and low SINR regions, e.g., 30 dB and 0 dB, is reduced. When the angular spread is 3 degrees, SINR degradation due to the arc-shaped null of the 2D Pattern is not distinguishable. In addition, except for the 3D Pattern-Wide, when the angular spread is 3 degrees and 5 degrees, it can be seen that this achieves almost the same distribution as the other patterns.

Figure 8 shows the SINR of the entire cell and the small

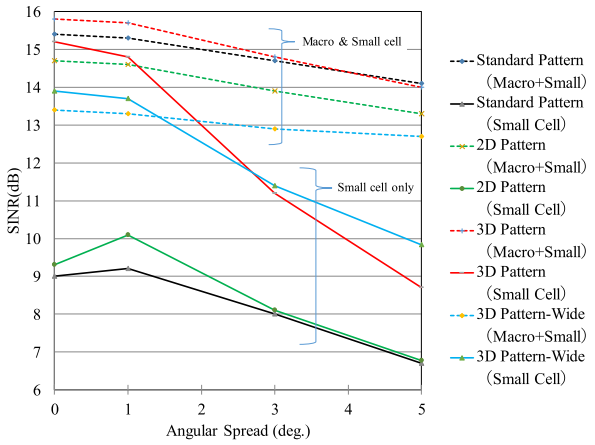

Fig. 8 SINR with angular spread.

cell only with the angular spread. The solid line represents the SINR of the small cell, and the dashed line represents the SINR of the entire cell. The SINR of the entire cell decreases 1–1.5 dB regardless of the pattern if the angular spread is from 0 to 5 degrees. For both the Standard Pattern and 2D Pattern, the SINR of the small cell decreases 2–2.5 dB. On the other hand, for the 3D Pattern and the 3D Pattern-Wide, the SINR decreases by 6.5 dB and 4 dB, respectively. These decreases are greater than those of the Standard Pattern and 2D Pattern because the null depth in the direction of the small cell becomes shallower due to the angular spread. However, the SINR of the 3D Pattern and the 3D Pattern-Wide is 2–3 dB larger than that for the Standard Pattern at an angular spread of 5 degrees. Therefore, the effect of the null pattern is confirmed.

Comparing the 3D Pattern and the 3D Pattern-Wide, if the angular spread is less than 1 degree, the SINR of the 3D Pattern is better than that of the 3D Pattern-Wide. If the angular spread is more than 3 degrees, the SINR of the 3D Patten-Wide is better than that of the 3D Pattern. These results shows that the narrow null pattern is suitable for rural and suburban areas and the wide null pattern is advantageous in urban and dense urban areas.

Generally, it is difficult to make broad and deep nulls on the antenna pattern at small number of antenna element. For that reason, in the case where the angular spread is small, the null of the narrow and deep is valid. On the other hand, in the case where the angular spread is large, the null of the wide and shallow is valid.

In this paper, the author shows the simulation results in a typical case. In a real environment, there are also many cases where there are multiple small cells in a variety of positions. The evaluation in some cases shows the results as in Ref. [23]. This reference shows that the Chebyshev pattern is effective to some extent in the case where two small cells are allocated to different positons.

4. Field Test

In the previous section, the effectiveness of the AAS antenna

(a) Overview

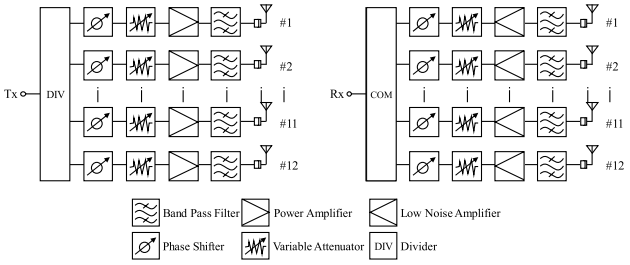

(b) RF block

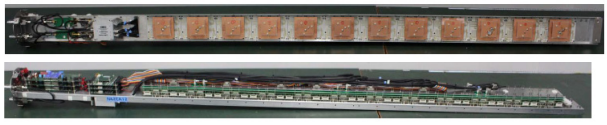

(c) Inside radome
top: front view bottom: side view

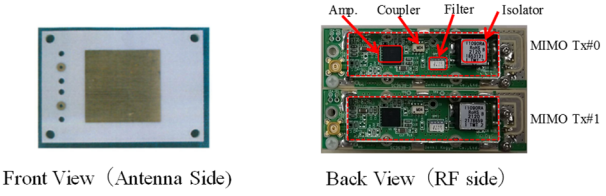

(d) Tx element of active antenna

Fig. 9 Views of the AAS.

pattern was simulated. In this section, the author demonstrates how the AAS can improve cell quality in a specific outdoor field test. The author used a 2 GHz band AAS that had been developed from basic research because the 3.5 GHz band had still not been licensed at the time the field test was conducted. For this reason, the parameters of this field test do not completely match those in the previous simulation section.

Figure 9(a) shows the appearance of the AAS; the frequency used is the 2 GHz band (3GPP band class 1). The antenna size is the same as that of a conventional 2 GHz band sector antenna, and the diameter and length are 135 mm and 2 m, respectively. In the radome, 12 self-diplexing antenna

Table 3 Specifications of the AAS.

Frequency Band	Tx: 2110-2130 MHz Rx: 1920-1940 MHz
Number of Array Elements	12-element linear array in vertical plane
MIMO	2-branch vertical/horizontal MIMO
Horizontal Beamwidth	80 degrees
Amplitude variable range of the elements	+3 dB/-3 dB (resolution: 0.1 dB)
Phase variable range of the elements	+180/-180 degrees (resolution 1 degree)

elements are arrayed with a distance of 120 mm between each element. The AAS incorporates the use of self-diplexing antenna elements that have been successfully miniaturized in the filter. The isolation between the transmission and reception bands of the self-diplexing antenna achieves more than 30 dB [19]. Further, this AAS has orthogonally polarized MIMO with corresponding vertical/horizontal polarization. Figure 9(b) shows the RF block system diagram of the AAS. Circuits such as the phase shifters and amplifiers are placed directly beneath the antenna elements; an amplitude of ±3 dB and a phase of ±180 degrees can be set. Figure 9(c) shows the front and back views inside the radome. In the front view, there are 12 antenna elements, and the part on the left side is the power supply. In the side view, the RF blocks are shown. Next, Fig. 9(d) shows an example of the tx antenna elements from the front and back view. There is small filters instead of a diplexer because the antenna type adopts a self-diplexing antenna. Also, because the transmitter power is low, RF parts can use mobile terminal parts. Therefore, it is possible to make this prototype AAS very compact.

Electrical tilt of a typical base station antenna is enabled by providing a phase shifter for each sub-array and changing the angle of the main beam. On the other hand, the AAS provides a phase shifter for each antenna element. As a result, in addition to the tilt of the main beam, flexible beam and null control can be performed. This flexible beam and null can be remotely controlled using an AISG interface [24]. AISG (Antenna Interface Standard Group) defines the international standard interface and protocol to control base station equipment including antennas. Table 3 shows the specification of this prototype AAS.

First, it is explained that the antenna patterns are adapted for the field testing environment. The up-tilt angle is 3 degrees because the target area is slightly higher than the location of the base station. Next, the null direction of the AAS is calculated based on the distance between the AAS and the small cell. Vertical patterns are created by an optimization algorithm that sets the mask pattern to satisfy the conditions in Table 4. In order to satisfy these conditions, the weight of the amplitudes and phases for the 12 antenna elements with vertical and horizontal polarization in the vertical plane are determined. The initial value of the amplitude weight is a uniform 0 dB, and the phase is initially 0 degree. The range is from −3 dB to 3 dB for the amplitude and from 0 to 360 degrees for the phase. Figure 10 shows that the optimization mask and initial antenna pattern of the AAS. The initial antenna pattern refers to the uniform pattern before the optimization.

Table 4 Optimization conditions.

	Upper sidelobe level	Main beam level	Null depth level
Target Value	< 5dB @ -80 ~ -10 deg.	> 17dB @ -3deg.	< -15dB @ 5 ~ 9deg.

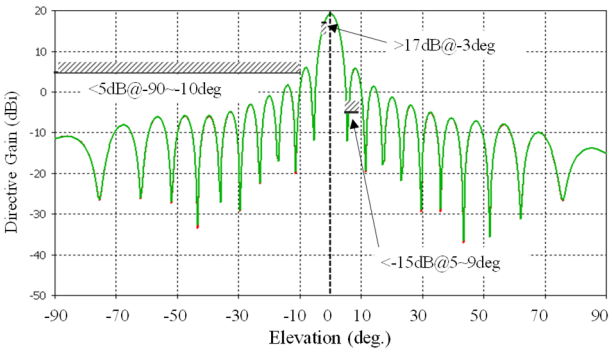

Fig. 10 Optimization mask of antenna pattern.

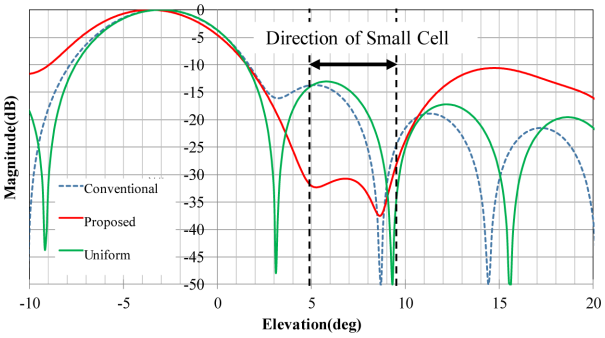

Fig. 11 Normalized antenna pattern in vertical plane.

Next, in order to decide the antenna weight, the optimization algorithms used are Nelder Mead Simplex and Trust Region, which are functions available in CST Design Studio [25]. The Nelder Mead Simplex algorithm is good for achieving convergence in the area of complex problems. If the number of parameters is small (5 or less), the number of iterations remains relatively small. The Trust Region algorithm can obtain an accurate result at high speed. It robustly converges, in a given parameter range, so it can obtain the optimum solution with a smaller number of iterations. On first step, the value is dynamically optimized using the Nelder Mead Simplex algorithm, then, if the result converges, the algorithm is changed to Trust Region as second step. The Trust Region algorithm is used to optimize to fine values. Some of the antenna patterns are shown in Fig. 11. The dashed line is a conventional antenna pattern [22] and the red line is the proposed optimized pattern. The proposed pattern does not partially satisfy the optimized mask shown in Fig. 10 at around −10 degrees on the elevation. However, the result can be ignored because it does not affect to the small cell. And, it is different to the antenna gain of some

Table 5 Field test conditions.

Cell Architecture	Frequency	2.0 GHz Band
	Cell Allocation	1 sector/macro cell 1 small cell
	Environment	3 degrees of the up slope from Macro Cell
Macro Cell Base Station	Antenna Height	30 m
	Antenna Gain	17 dBi
	EIRP	46 dBm
Small Cell Base Station	Antenna Pattern	Omni-directional
	Antenna Height	5 m
	Antenna Gain	2 dBi
	EIRP	23 dBm
Terminal Station	Antenna Pattern	Omni-directional
	Antenna Height	1.5 m
	Antenna Gain	0 dBi

antenna patterns, however, the antenna pattern of Fig. 11 is normalized to align the effective isotropic radiated power (EIRP) by the AAS amplitude adjustment function within +1 dB/−1 dB.

The distance from the AAS to the small cell is 220 m in direct line of sight, and this point is located 7 degrees down in the elevation plane. The radius of the small cell is defined as 100 m. For that reason, the direction the small cell is within from 5 to 10 degrees. The height of the base station is 30 m. From Fig. 11, the level of magnitude difference between the conventional and proposed patterns is approximately 15 dB. This value is sufficient to expect an improvement of the SINR in the small cell area.

4.1 Field Test Environment

To confirm the null pattern transmission by the AAS from the macro cell to the small cell, the author carried out field tests in Tochigi prefecture. The AAS used in the field tests has an array of 12 active antenna elements in the vertical plane, which are composites of amplifiers and filters [19]. Table 5 shows the field test conditions. The AAS antenna pattern is as shown in Fig. 11. The pattern variables are remotely controlled using the AISG interface and protocol.

In this field test, the null pattern is in an arc-shaped formation that was shown as the 2D Pattern in the previous section, because there is only one antenna array in the horizontal plane. Originally, the spot null was considered desirable for the small cell area, but in this case, this arc-shaped null pattern was evaluated.

4.2 Results of Field Test

Measurement data were collected inside an area about 800 m from the base station of the macro cell by conducting a drive test in a suburban area. Data were collected by the terminal station on the vehicle at 1-second intervals.

Figure 12(a) shows the cumulative distribution of SINR of the macro cells and small cells, and (b) shows the SINR for the small cells only.

From Fig. 12(a), the uniform and proposed patterns are

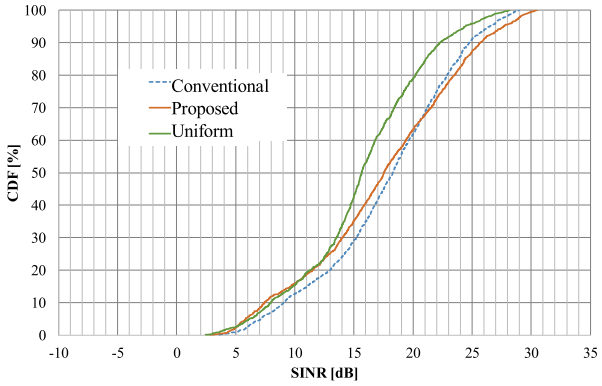

(a) SINR for entire area

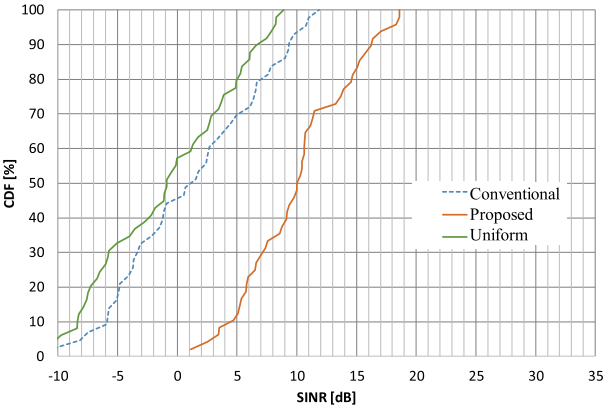

(b) SINR for small cell area

Fig. 12 SINR in entire and small cell area.

approximately 2 dB lower than the conventional pattern at 50% of the CDF (cumulative distribution function). Next, from Fig. 12(b), the proposed antenna pattern is 9 dB and 7.5 dB better than the uniform and conventional patterns, respectively. And, the peak SINR of the proposed pattern is able to achieve 18 dB. These reason for the improvement when using the proposed pattern is the effect of the null pattern transmission from the AAS to the small cell.

In conclusion, it is indicated that it is possible to improve the cell quality by proposed AAS.

5. Conclusion

This paper reported on next-generation antenna technology, in particular, on the evaluation of AAS technology to develop Massive MIMO.

First, in order to solve the interference due to the same frequency being used by the macro cell and the small cell, the paper focused on the AAS beam and null control function. An area simulation was carried out for three sectors with one small cell per sector. It was found that the SINR of the small cell improved by 6 dB using AAS beam and null control. Moreover, when considering the angular spread, it was found that a narrow null pattern is suitable in rural and

suburban areas, while a wide null pattern is advantageous in urban and dense urban areas.

In addition, field tests were performed. The results showed that the maximum improvement in the SINR of 9 dB is obtained in suburban areas. Thus, this paper shows that it is possible to dynamically improve the SINR by the AAS, and this improvement of SINR enables high-speed data transmission in wireless communication systems to be achieved.

In the future, spectrum utilization for frequency reuse by antenna technologies will be more important. The purpose of this paper is to assist similar studies in the future.

Acknowledgments

The author gratefully acknowledges the assistance of Dr. Ichiro Oshima, Mr. Keisuke Sato and Mr. Yukitaka Takahashi from Denki Kogyo Co., Ltd., particularly for their help with some of the field tests and manufacturing.

References

[1] H. Arai and K. Cho, "Cellular and PHS base station antenna system," IEICE Trans. Commun., vol.E86-B, no.3, pp.980–992, March 2003.
[2] S. Nanba, N. Miyazaki, Y. Hirota, and Y. Kishi, "MIMO capacity estimation based on single and dual-polarization MIMO channel measurements," APCC 2010, pp.313–318, Oct. 31–Nov. 3 2010.
[3] S. Ko, Y. Lee, K. Baek, Y. Kim, and W. Hong, "Low profile PCB integrated mmWave array antenna solutions for 5G mobile communication," 3rd AWAP2016, p.33, Centum Hotel in Busan, Korea, Jan. 2016
[4] H. So, A. Ando, T. Seki, M. Kawashima, and T. Sugiyama, "Multi-band sector antenna with same beamwidth employing multiple woodpile metamaterial reflectors," IEICE Trans. Electron., vol.E97-C, no.10, pp.976–985, Oct. 2014.
[5] R. Wongsan, P. Krachodnok, and P. Kamphikul, "A sector antenna for mobile base station using MSA array with curved woodpile EBG," Open Journal of Antennas and Propagation, 2014, vol.2, no.1, pp.1–8, Published Online March 2014 in SciRes.
[6] I. Oshima, T. Seki, N. Michishita, and K. Cho, "Omnidirectional composite right/left-handed leaky-wave antenna with downtilted beam," IEEE AP-S 2015, Paper THP-A1.1A.6, pp.2439–2440, 2015.
[7] I. Oshima, "Development of base station antennas for 5G mobile communication systems," IEEE iWEM2016, TU1A, pp.1–2, 2016.
[8] F. Hyjazie, P. Watson, and H. Boutayeb, "Dual band interleaved base station phased array antenna with optimized cross-dipole and EBG/AMC structure," AP-S 2014 IEEE, pp.1558–1559, 2014.
[9] H. Boutayeb, J.P. Daniel, F. Gadot, P.Y. Garel, A. de Lustrac, K. Mahdjoubi, P. Ratajczak, K. Sayegrih, and A.C. Tarot, "New beam steering base station antenna using EBG material," ISAP2014 4D3-2, pp.1325–1328, 2014.
[10] K. Cho, H. So, and A. Ando, "HPBW control of dipole antenna with frequency selective reflector using different size elements," IEICE Communication Express, vol.5, no.3, pp.90–94, 2016.
[11] T. Nakamura, A. Benjebbour, Y. Kishiyama, S. Suyama, and T. Imai, "5G radio access: Requirement, concept and experimental trials," IEICE Trans. Commun., vol.E98-B, no.8, pp.1397–1406, Aug. 2015.
[12] H. Papadopoulos, C. Wang, O. Busalioflu, X. Hou, and Y. Kishiyama, "Massive MIMO technologies and challenges towards 5G," IEICE Trans. Commun., vol.E90-B, no.3, pp.602–621, March 2016.
[13] K. Nishimori, "Multi-beam massive MIMO using analog-digital hybrid configuration," 3rd AWAP2016, pp.34–35, Centum Hotel in Busan, Korea, Jan. 2016.
[14] M. Nakano, H. Ishikawa, and S. Nomoto, "Small-sized shaped beam base station antenna with superior intersector interference reduction in high speed cellular systems," IEICE Trans. Commun., vol.E93-B, no.10, pp.2586–2594 Oct. 2010.
[15] H. Shimodaira, G.K. Tran, K. Sakaguchi, K. Araki, S. Kaneko, N. Miyazaki, S. Konishi, and Y. Kishi, "Optimization of picocell location and its parameters in heterogeneous networks with hotspot," IEICE Trans. Commun., vol.E96-B, no.6, pp.1338–1347, June 2013.
[16] X. Li, T. Bai, and R.W. Heath, Jr., "Impact of 3D base station antenna in random heterogeneous cellular networks," IEEE WCNC'14 Track3 pp.2254–2259, 2014.
[17] S. Yoshida, T. Kawamura, T. Ihara, M. Murakami, and N. Miyadai, "Field trial of active antenna system in LTE — Configurations of field trial base station and downlink performance evaluations," Proc. Commun. Conf. IEICE 2014, B-1-151, 2014 (in Japanese).
[18] C.-H. Ko, K.M.J. Ho, and G.M. Rebeiz, "An electronically-scanned 1.8–2.1 GHz base-station antenna using packaged high-reliability RF MEMS phase shifters," IEEE Trans. Microwave Theory Techn., vol.61, no.2, pp.979–984, Feb. 2013.
[19] K. Sato, S. Natori, I. Oshima, T. Kitayabu, M. Nakano, K. Miyata, H. Hayashi, and K. Gosui, "Active array antenna system for cellular base station," IEICE Technical Report, AP2015-65, 2015 (in Japanese).
[20] "OTA measurement method for output power," 3GPP TSG-RAN Working Group 4 (Radio) Meeting #69, R4-135870, San Fransisco, USA, 11th–15th, Nov. 2013.
[21] M. Nakano, T. Kitayabu, S. Natori, K. Sato, I. Oshima, K. Miyata, H. Hayashi, and K. Gosui, "Field evaluation of cell quality by beam control with active array antenna system," IEICE Technical Report, AP2015-90, 2015 (in Japanese).
[22] M. Nakano and K. Kobayashi, "Antenna pattern and quality of cell — Sidelobe and nullfill evaluation", Proc. Commun. Conf. IEICE 2007, B-1-13, 2007 (in Japanese).
[23] M. Nakano, T. Kitayabu, K. Sato, and I. Oshima, "Simulation evaluation of cell quality by beam control on active array antenna system," IEICE Technical Report, AP2016-30, 2016 (in Japanese).
[24] http://www.aisg.org.uk/
[25] CST STUDIO, http://www.aetjapan.com/software/CST_Overview.php

Masayuki Nakano received his B.E. and M.E and Ph.D degrees in electrical and computer engineering from Yokohama National University, in 1990, 1992 and 2011, respectively. In 1992, he worked for IDO Corporation and in 2001 he was an employee of KDDI Corporation. In 2007, he joined KDDI R&D Laboratories Inc. His research interests are in cellular antenna and propagation and the IMT-Advanced, Mobile WiMAX system and next generation systems. He was the recipient of the "Meritorious Award on Radio" conferred by the Association of Radio Industries and Businesses for the development of polarization diversity antenna for base stations in 1997, for the development of the DOA estimation system and in 2006 and for the development of shaped beam base station antenna in 2013. He served as Secretary of Technical Group on Antenna and Propagation of IEICE from 2014 to 2015. He is a member of IEEE.